ACS POLYMERS Au
AN OPEN ACCESS JOURNAL OF THE AMERICAN CHEMICAL SOCIETY

pubs.acs.org/polymerau

Article

Effect of pH on the Properties of Hydrogels Cross-Linked via Dynamic Thia-Michael Addition Bonds

Thomas M. FitzSimons, Eric V. Anslyn, and Adrianne M. Rosales*

Cite This: *ACS Polym. Au* 2022, 2, 129–136

Read Online

ACCESS | Metrics & More | Article Recommendations | Supporting Information

ABSTRACT: Hydrogels cross-linked with dynamic covalent bonds exhibit time-dependent properties, making them an advantageous platform for applications ranging from biomaterials to self-healing networks. However, the relationship between the cross-link exchange kinetics, material properties, and stability of these platforms is not fully understood, especially upon addition of external stimuli. In this work, pH was used as a handle to manipulate cross-link exchange kinetics and control the resulting hydrogel mechanics and stability in a physiologically relevant window. Poly(ethylene glycol)-based hydrogels were cross-linked with a reversible thia-Michael addition reaction in aqueous buffer between pH 3 and pH 7. The rate constants of bond exchange and equilibrium constants were determined for each pH value, and these data were correlated with the resulting mechanical profiles of the bulk hydrogels. With increasing pH, both the forward and the reverse rate constants increased, while the equilibrium constant decreased. These changes led to faster stress relaxation and less stiff hydrogels at more basic pH values. The elevated pH values also led to an increased mass loss and a faster rate of release of an encapsulated model bovine serum albumin fluorescent protein. The connection between the kinetics, mechanics, and molecular release profiles provides important insight into the structure–property relationships of dynamic covalent hydrogels, and this system offers a promising platform for controlled release between physiologically relevant pH values.

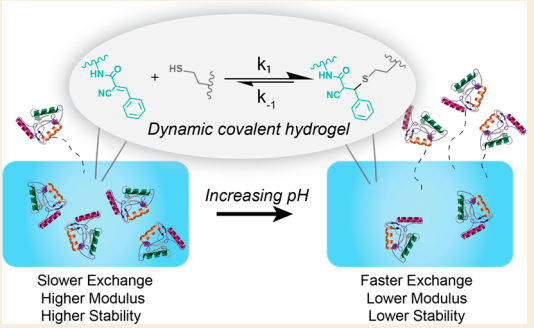

KEYWORDS: *hydrogel, viscoelastic, self-healing, biomaterial, release, dynamic covalent, thia-Michael*

INTRODUCTION

Dynamic covalent polymeric networks have attracted recent attention for a variety of applications, including drug delivery systems,[1−3] self-healing materials,[4−6] and pressure-sensitive adhesives.[7,8] Because dynamic covalent reactions are reversible, their use in polymeric networks gives rise to materials with properties that change on time scales relative to bond exchange kinetics.[9] These bond exchange kinetics are directly related to molecular structure and bond type. For instance, previous work with reversible thiol-ene networks leveraged chemical modifications to the aromatic ring at the β site of an α,β-unsaturated carbonyl to induce a preferential change in the forward rate constant.[4,10] Specifically, more electron-withdrawing substituents increased the forward rate constant, leading to larger storage moduli for the resulting networks. However, external stimuli, such as catalyst addition or temperature, also offer a route to directly manipulate material properties via bond exchange kinetic control.[1,11−14] In dynamic covalent hydrogel systems, in particular, responsive materials may be further manipulated through the control of pH.

Several dynamic covalent reactions rely on a deprotonation event for either bond formation (forward direction), bond breaking (reverse direction), or both. Manipulation of pH allows the user to control the thermodynamics of these deprotonation events, which thereby affects the kinetics of bond exchange that rely on those events. Importantly, whether the bond exchange kinetics are increased or decreased with pH depends on the reaction mechanism for that system. For instance, in a bisaliphatic hydrazone cross-linked hydrogel, increasing pH led to an initial increase in the gelation speed up to physiological pH, after which the gelation speed began to decrease.[15] To explain this, McKinnon et al. found that the forward rate constant for the hydrazone formation reaction reached a maximum at physiological pH. In two other studies using boronic ester cross-linked hydrogels, however, increasing pH slowed the reverse reaction rate constant, leading to more stable and elastic hydrogels at alkaline conditions.[2,16] Clearly, the individual response of the forward and reverse cross-linking reactions plays a key role in how a dynamic covalent hydrogel responds to changes in pH.

Received: October 29, 2021
Revised: December 9, 2021
Accepted: December 13, 2021
Published: December 28, 2021

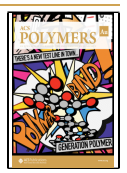

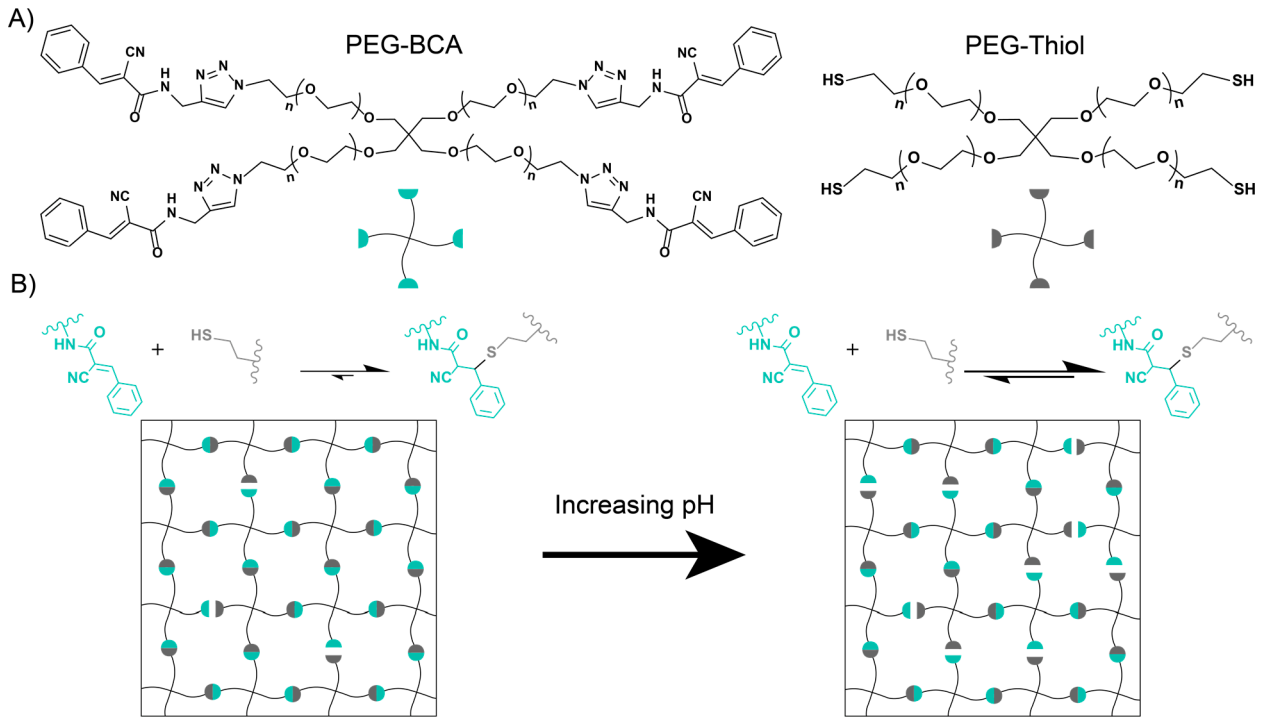

Figure 1. (A) Chemical structures for the two macromers used in this study. The conjugate acceptor is a four-arm benzylcyanoacetamide-functionalized poly(ethylene glycol) (PEG-BCA). The nucleophile is a four-arm PEG-thiol. (B) Schematic of the effect pH plays on the reaction. With increasing pH, both the forward and reverse rate constants increase, while the equilibrium constant decreases.

A key application that has utilized pH responsiveness is drug delivery systems, which exhibit different release profiles of encapsulated therapeutics when hydrogel mesh size changes upon physiologically relevant shifts in pH. Many of these systems are polyelectrolytes and therefore respond by changes in swelling behavior due to ionic interactions.[17−21] Dynamic covalent hydrogels, however, need not be polyelectrolytes to exhibit differential release profiles when changing pH. For instance, in hydrazone cross-linked polyacrylamide-based hydrogels, Rhodamine B was released more quickly at pH 2.5 than at pH 6 or pH 7.4.[22] These differences in release were attributed to the hydrogel stability; at pH 2.5, the hydrogel quickly degraded due to the lability of the hydrazone bonds, whereas the hydrogels were more stable at elevated pH, allowing for sustained release. Further work is needed to understand the relationship between hydrogel stability and release as a function of pH in dynamic covalent systems to enable delivery applications for encapsulated therapeutics.[23,24]

Toward that end, we investigated the effect of pH on the properties of a dynamic covalent hydrogel cross-linked with a reversible thia-Michael addition reaction. Utilizing a benzyl-cyanoacetamide-functionalized four-arm poly(ethylene glycol) (PEG-BCA) macromer (Figure 1A), we measured the reaction progress for pH 3−7 via UV/vis spectroscopy and determined the forward and reverse rate constants by fitting a second-order kinetic model. By combining the PEG-BCA with a four-arm PEG-thiol macromer, we also assessed the effect of these kinetic changes on the mechanics of the formed hydrogels by shear rheometry, as well as the ability for these hydrogels to self-heal at different pH values (Figure 1B). We specifically selected pH values between 3 and 7 to span the range in the gastrointestinal tract, which is of interest for many oral delivery applications. Finally, we characterized the mass loss behavior for these hydrogels between pH 3 and pH 7, as well as measured the release profiles of an encapsulated model protein. Taken together, this study offers insight into the behavior of a pH-responsive dynamic covalent hydrogel with potential applications in therapeutic delivery for the gastrointestinal tract.

MATERIALS AND METHODS

All materials were used as purchased unless otherwise specified. Propargyl amine, anhydrous ethanol, peptide synthesis grade dimethylformamide (DMF), dimethyl sulfoxide-d_6 (DMSO-d_6), deuterium oxide, deuterated chloroform, Sigmacote, copper sulfate, sodium ascorbate, and β-mercaptoethanol were purchased from Sigma-Aldrich. Four-arm 20 kDa molecular weight PEG-azide and four-arm 10 kDa molecular weight PEG-thiol were purchased from JenKem USA. Methyl cyanoacetate, diethyl ether, and citric acid were purchased from Fisher Scientific.

Synthesis of Propargyl Cyanoacetamide

Propargyl cyanoacetamide was synthesized as previously described.[4] Briefly, propargyl amine (5.81 mL, 0.0908 mol, 1.0 equiv) and methyl cyanoacetate (8.01 mL, 0.0908 mol, 1.0 equiv) were added to an oven-dried round-bottom flask. The reaction proceeded upon stirring for 24 h at room temperature. The product precipitated out and was washed with 200 mL of ice-cold diethyl ether under vacuum filtration. The product was a light yellow solid, yield = 84% (Figure S1). ^{1}H NMR (DMSO-d_6, 400 MHz): δ 8.66 (t, 1H), 3.86 (dd, 2H), 3.62 (s, 2H), 3.14 (t, 1H). HRMS (CI) $[M + H]^+$ calcd 123.06; found, 123.0558.

Synthesis of PEG-Cyanoacetamide (PEG-CA)

PEG-CA was synthesized via copper-catalyzed click chemistry as previously described.[4] Briefly, four-arm, 10 kDa molecular weight PEG-azide (1 g, 0.1 mmol) and propargyl cyanoacetamide (58.62 mg, 0.48 mmol, 4.8 equiv) were added to a round-bottom flask. This flask was purged with argon for 5 min. Copper(II) sulfate (12.77 mg, 0.08 mmol, 0.8 equiv) and sodium ascorbate (31.7 mg, 0.16 mmol, 1.6 equiv) were added to a separate vial, which was also purged with argon. Ultrafiltered water (8 mL) and peptide synthesis grade DMF

https://doi.org/10.1021/acspolymersau.1c00049
ACS Polym. Au 2022, 2, 129−136

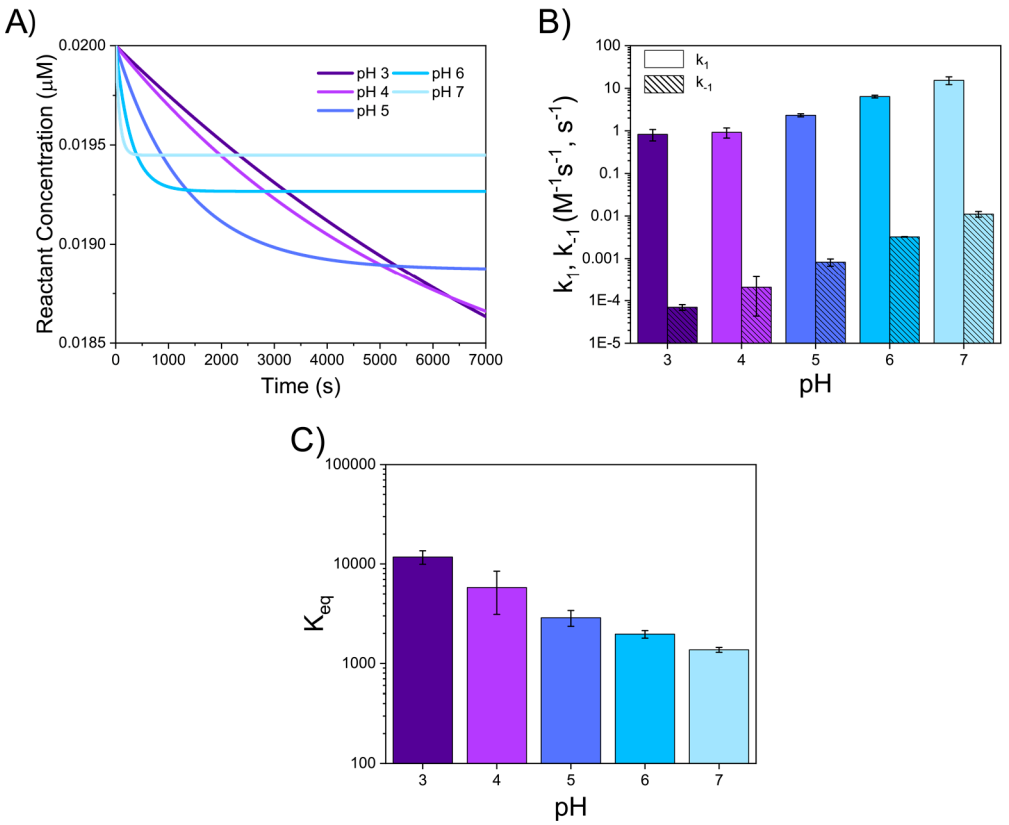

Figure 2. (A) Representative second-order kinetic model fits for each pH value for the disappearance of reactants. As the pH increases, the equilibrium is reached at a higher reactant concentration but is achieved faster. (B) Forward and reverse rate constants for each pH. As the pH increases, both the forward and reverse rate constants increase. (C) Equilibrium constants for each pH. As both rate constants increase with increasing pH, the reverse rate constant must be increasing faster in order for the equilibrium constant to decrease.

(8 mL) were added via syringe to the vial containing copper sulfate and sodium ascorbate. The vial was sonicated to dissolve the solids. This vial was cannulated to the flask containing the PEG and propargyl cyanoacetamide. The mixture was allowed to react for 3 days under a constant flow of argon. After 3 days, the contents were precipitated into ice-cold diethyl ether (two vials with 30 mL of ether each). The reaction mixture phase-separated into a PEG-containing aqueous layer and an organic layer. The organic layer was discarded, and the aqueous layer was moved through a 0.2 μm PTFE syringe filter into a dialysis bag (1 kDa MWCO) and dialyzed against deionized water for 3 days, changing the water every day. After 3 days, the contents were lyophilized. Yield = 99%, functionalization = ~92% (Figure S2). ^{1}H NMR (DMSO-d_6, 400 MHz): δ 8.68 (t, 1H), 7.92 (s, 1H), 4.46 (t, 2H), 4.28 (d, 2H), 3.4 (s, 227H).

Synthesis of Conjugate Acceptor-Functionalized PEG (PEG-BCA)

A Knoevenagel condensation was used to attach a benzaldehyde to PEG-CA to make PEG-BCA, as previously described.[4] PEG-CA (272 mg, 0.0272 mmol), anhydrous ethanol (5 mL), and benzaldehyde (1.1 mL, 10.88 mmol, 400 equiv) were added to a round-bottom flask. The flask was purged with argon for 5 min and then heated to 65 °C. The reaction was allowed to proceed for 2 days. After 2 days, the solution was precipitated through a 0.2 μm PTFE syringe filter into ice-cold diethyl ether (35 mL, three times, filtering only the first time) to separate the functionalized PEG product from excess aldehyde. After each precipitation, the vial was centrifuged to recover the precipitated solid PEG product, and the supernatant was discarded. After precipitation, the solid product was dried overnight under vacuum. Yield = 99%, functionalization = ~91% (Figure S3). ^{1}H NMR (DMSO-d_6, 400 MHz): δ 8.99 (t, 1H), 8.17 (s, 1H), 7.94 (s, 1H), 7.89 (dd, 2H), 7.51−7.56 (m, 3H), δ = 3.4 (s, 227H).

Rheometry

Rheometry experiments were conducted using a TA Instruments Discovery HR2 rheometer. An 8 mm flat stainless-steel geometry on a stainless-steel Peltier plate was used for all experiments unless otherwise stated. Hydrogels were preformed in 8 mm molds. Hydrogels were surrounded with light mineral oil after lowering the geometry to the experimental gap height to prevent dehydration. All experiments were done at 25 °C. Frequency sweeps were performed from 0.01 to 10 rad/s at 1% strain. The step strain experiment was performed at 10 rad/s using a 20 mm 2° stainless-steel cone geometry, using 1% and 1000% strains.

UV/Vis Spectroscopy

Kinetic rate constants were determined via absorbance on a QE Pro high-performance spectrometer manufactured by Ocean Insight. First, an open top glass cuvette was filled with 1 mL of a 40 μM solution of the conjugate acceptor in citric acid buffer. A small stir bar was added. The absorbance was recorded, and an additional 1 mL of a 40 μM solution of β-mercaptoethanol in citric acid buffer was added. This led to an initial concentration for both molecules of 20 μM. The concentration of each species in time was calculated based on the extinction coefficient from the start of the experiment when there is no product, using a procedure from a previous study.[4] The concentration of the conjugate acceptor was plotted versus time and fit to a second-order kinetic model that incorporates a first-order reverse reaction to determine the forward and reverse rate constants (eq S1). This model assumes equal starting concentrations of both reactants in order to provide an analytical solution to the differential equation for the rate of change of the concentrations. An in-depth description of this model is provided in the Supporting Information.

https://doi.org/10.1021/acspolymersau.1c00049
ACS Polym. Au 2022, 2, 129−136

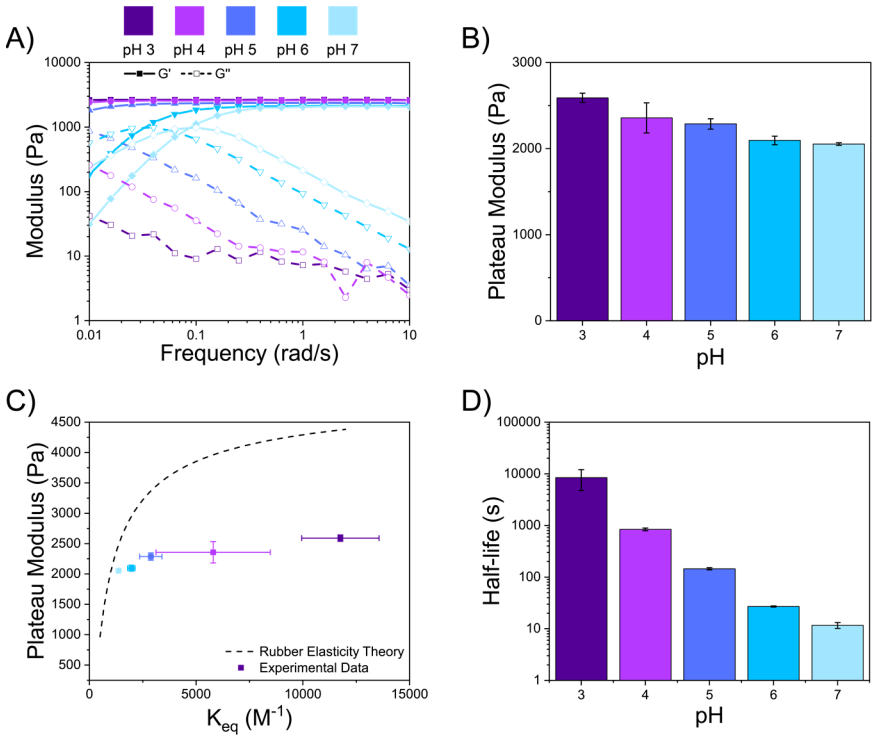

Figure 3. (A) Representative frequency sweep graphs for each pH value. As the pH increases, so too does the crossover point. The lower pH values had crossover points below the measurable range on the rheometer. (B) Plateau modulus for each pH value. As pH increases, the plateau modulus decreases, mirroring the behavior of the equilibrium constant. (C) Plateau modulus versus equilibrium constant. Also included is theoretical data based on modified rubber elasticity theory with calculations developed on theory by Parada and Zhao[28] on ideal reversible polymer networks. (D) Stress relaxation half-life for each pH value. As the pH increases, the half-life of stress relaxation decreases.

NMR Spectroscopy

^{1}H NMR spectra (400 MHz) were recorded on an Agilent MR400 spectrometer at room temperature.

Hydrogel Preparation for Rheometry

All hydrogels were formulated at room temperature by mixing PEG-BCA with a 1:1 stoichiometric amount of thiol-functionalized four-arm 10 kDa PEG. Unless otherwise stated, the hydrogels contained 5 wt % polymer with a functional group concentration around ∼9.5 mM.

Hydrogels for rheometry were made in cylindrical molds with an 8 mm diameter from 0.5 mm thick silicone sheets. The silicone molds were placed on a Sigmacote-treated hydrophobic glass slide. The two macromer solutions were pipet mixed in the molds, and another Sigmacote-treated glass slide was placed on top of the mold. After gelation, each hydrogel was used for rheometry.

Mass Loss Hydrogel Preparation

Hydrogels for the swelling unrestricted mass loss study were made in 5 mm diameter syringes with the end cut off. The two macromers were pipet mixed in the barrel of the syringe, and parafilm was placed over each syringe to prevent dehydration. After gelation, hydrogels were ejected from the syringe barrel and used for the experiment. Each hydrogel had a volume of 100 μL.

Hydrogels for the swelling restricted mass loss study were made in the bottom of 1.5 mL microcentrifuge tubes. The two macromers were pipet mixed in the tubes and briefly centrifuged to make sure the hydrogels were in the bottom of the tubes. After gelation, the hydrogels were ready for the experiment, wherein 1.3 mL of buffer was placed on top of each hydrogel. Each hydrogel had a volume of 50 μL.

Protein Release Study

In the protein release study, the hydrogels were prepared in an identical manner to the swelling restricted mass loss study, but the macromer solutions contained 2.5 mg/mL of bovine serum albumin (BSA)-fluorescein, which was encapsulated in the hydrogels upon gelation. Then, 1.3 mL of buffer with no protein was added to each tube, and 100 μL aliquots were taken at each time point, with the taken volume being replaced by fresh buffer. The aliquot's fluorescence was determined using a plate reader, and the concentration of the protein was determined based on a standard curve (Figure S4). The excitation and emission wavelengths were 494 nm and 520 nm, respectively.

RESULTS AND DISCUSSION

pH Affects Bond Exchange Kinetics

To probe the effects of pH on the kinetics of the reversible thia-Michael addition reaction, we measured the rate constants over the pH range of 3−7 via UV/vis spectroscopy. Specifically, we mixed PEG-BCA with an equimolar concentration of β-mercaptoethanol, a small molecule thiol, and monitored the disappearance of the α,β-unsaturated carbonyl peak as a function of time (Figure S5). Due to the conjugation across this double bond, the conjugate acceptor molecule absorbs light strongly at a wavelength of 300 nm, while the product and thiol do not. We assumed the conjugate acceptor and thiol only reacted with each other, and that there were no side reactions present, which is a reasonable assumption given the "click" nature of the Michael addition reaction.[25] Thus, the Beer−Lambert law was used to calculate the concentrations of both reactants and products. The resulting concentration values were then fit to a second-order reversible addition kinetic model to determine the forward and reverse rate constants (Figure 2A).[26] This experiment was repeated for each pH value between pH 3 and pH 7, each using citric acid as the buffer. The reactant concentration decreased faster for

https://doi.org/10.1021/acspolymersau.1c00049
ACS Polym. Au 2022, 2, 129−136

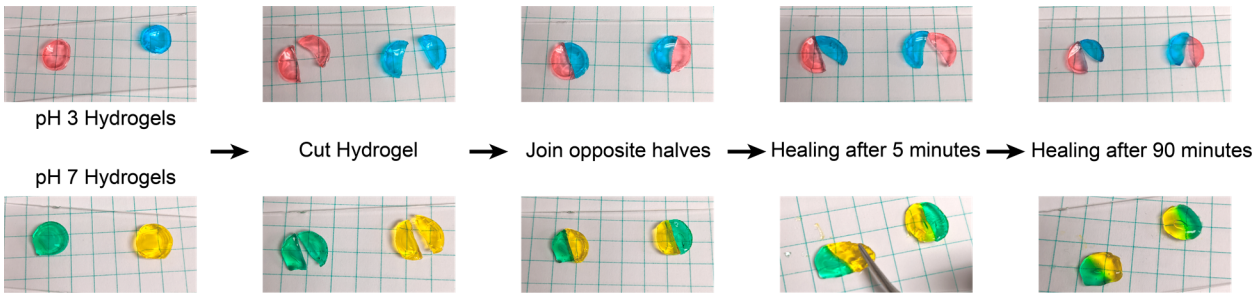

Figure 4. Self-healing ability for pH 3 (top) or pH 7 (bottom) hydrogels. Two hydrogels for each pH were dyed, cut, and the opposing halves were joined. After 5 min, the pH 7 hydrogels healed the defect, and after 90 min, the pH 3 hydrogels were still unhealed.

the higher pH values but stabilized at a higher concentration upon reaching equilibrium.

The faster decrease in the reactant concentration for higher pH values signified larger forward rate constants (Figure 2B). Indeed, model fits indicated that the forward rate constant increased from 0.83 M^{-1} s^{-1} at pH 3 to 15.3 M^{-1} s^{-1} at pH 7. These results agree with the proposed mechanism for the reaction (Figure S6), which involves deprotonation of the thiol for the forward direction. Interestingly, however, the proposed mechanism also indicates a deprotonation event for the reverse reaction to generate an enolate, thereby indicating that an increase in pH would increase both rate constants. What is less apparent, however, is which reaction direction is more strongly affected and how pH affects the resulting equilibrium constant for this reaction. Indeed, our calculated values for the reverse rate constant also increased with pH, from 6.24×10^{-5} s^{-1} at pH 3 to 1.1×10^{-2} s^{-1} at pH 7 (Figure 2B). Relative to the forward rate constant (~23-fold increase with pH), the reverse rate constant was more strongly affected by pH (~176-fold increase). Thus, the equilibrium constant decreased for more basic pH, resulting in values from 1.05×10^{4} M^{-1} at pH 3 to 1.37×10^{3} M^{-1} at pH 7 (Figure 2C). These results explain the higher plateau values of the reactant concentrations at elevated pH seen in our kinetic experiments.

Impact of pH on Hydrogel Mechanics

We anticipated that a decrease in the equilibrium constant with increasing pH would correspond to a decrease in the plateau storage moduli of hydrogels formed from PEG-BCA and PEG-thiol. To test this hypothesis, we formulated hydrogels at a PEG concentration of 5 wt % and 1:1 thiol-ene stoichiometry. Shear storage moduli were measured using an oscillatory rheometer at 1% strain and a frequency of 1 rad/s (Figure 3A), which is within the linear viscoelastic regime (Figure S7). We observed a small decrease in the plateau moduli of the hydrogels from an average of 2590 Pa at pH 3 to 2050 Pa at pH 7 (Figure 3B). The decrease in equilibrium constant translates to a lower cross-linking density as the cross-linking reaction is shifted toward the reactants. This trend can be predicted by modified rubber elasticity theory, which incorporates the equilibrium constant in calculations of the hydrogel cross-link density (Table S1).

We specifically compared our results to those derived from rubber elasticity theory that used a model for cross-link density in ideal reversible networks developed by Parada and Zhao.[16,27,28] This model predicts increasing plateau moduli as the equilibrium constant increases, which matches the trend seen in our results (Figure 3C). Furthermore, the model indicates that the gains in the plateau modulus taper as the equilibrium constant becomes sufficiently high. In other words, as the cross-linking reaction approaches high conversion (~79% at pH 5 for our system, based on the equilibrium constant), there are diminishing returns on the number of new elastically active chains. Our results mirrored this diminished effect of high K_{eq} on the plateau modulus. Although the predicted trend matched our results, our measurements yielded lower values of the storage modulus compared to the theory, indicating that more defects may be present than those accounted for by the model.

Interestingly, while the plateau storage moduli decreased slightly with pH, the crossover point of G' and G'' showed a large increase from pH 3 to pH 7, which is consistent with the increase in the reverse rate constant (Figure S8). Because the bonds are reversible, a sufficiently slow rotational frequency allows the bonds to rearrange fast enough to dissipate a majority of any stored energy in the polymer backbone. This behavior is demonstrated in the low-frequency regions when the shear loss modulus is higher than the shear storage modulus, indicating a viscoelastic liquid (Figure 3A). As demonstrated by the kinetic rate data, a more acidic pH significantly slows the reaction, meaning that the bonds rearrange on a longer time scale. Thus, the hydrogels with slower bond exchange kinetics displayed more elastic behavior at low frequencies, and the crossover point decreased significantly. In fact, the crossover points at pH 3 and pH 4 were small enough to be outside the measurement range of the rheometer. Thus, to better understand how the bond exchange rate of the cross-links impacts hydrogel properties, we performed stress relaxation experiments (Figure S9). The breaking and re-forming of bonds allows the network to dissipate stress, and the half-life of this dissipation is directly related to the kinetics of the cross-linking reaction. The half-life of stress relaxation decreased from 8410 s at pH 3 to 11.7 s at pH 7 (Figure 3D), indicating faster exchange in the networks at elevated pH.

To demonstrate the pH effects on the bond exchange rate on the bulk scale, we performed self-healing experiments. Because the bonds are dynamic, when a defect in the network occurs, cross-links can break and re-form across the defect. The time scale of this repair depends on the rate constants for the cross-linking reaction. In the case of these hydrogels, higher pH values corresponded to a relatively rapid exchange of cross-links, while lower pH values corresponded to a severely decreased rate of cross-link exchange. We therefore fabricated two sets of hydrogels: (1) two hydrogels at pH 3 and (2) two hydrogels at pH 7 (Figure 4). Each hydrogel was dyed a separate color. The hydrogels were then cut in half and matched with the half made at the same pH. After 5 min, the hydrogels formed at pH 3 demonstrated no self-healing,

https://doi.org/10.1021/acspolymersau.1c00049
ACS Polym. Au 2022, 2, 129−136

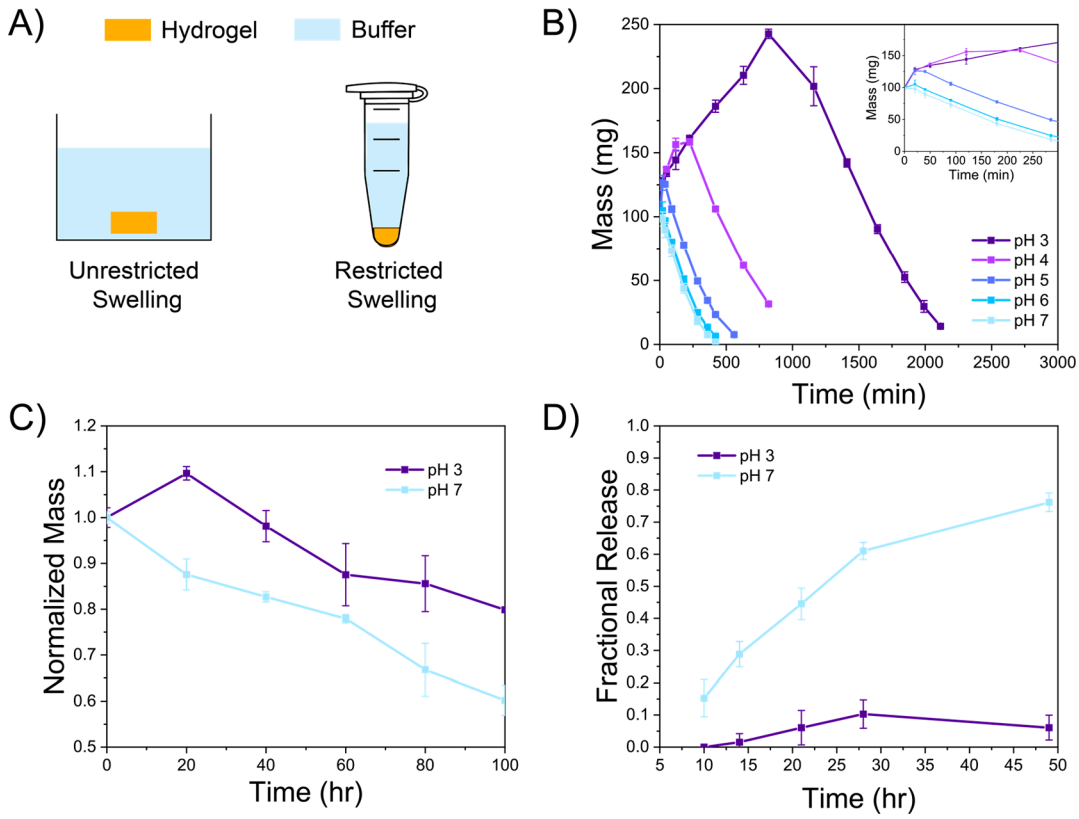

Figure 5. (A) Schematic for the two mass loss studies. In the unrestricted swelling test, a hydrogel was placed in a bath of buffer. In the restricted swelling test, a hydrogel was formed in the bottom of a microcentrifuge tube. (B) Unrestricted swelling mass loss study. As the pH increases, the hydrogel fully dissolves in a shorter amount of time. The inset shows the first 300 min of the study, highlighting that the maximum swollen mass decreases as the pH increases. (C) Swelling restricted mass loss. This restriction dramatically increases the amount of time the hydrogels take to dissolve into solution. The pH 7 hydrogels still lost mass at a faster rate than the pH 3 hydrogels. (D) Encapsulated BSA tagged with fluorescein was released from either a pH 3 or a pH 7 hydrogel over time. The pH 7 hydrogel released the encapsulated protein at a significantly faster rate.

whereas the hydrogels formed at pH 7 clearly rejoined across the defect. Furthermore, after 90 min, the hydrogels formed at pH 3 remained unhealed. Additionally, a step strain experiment was performed on both the pH 3 and the pH 7 hydrogels (Figure S10). On a 2° cone geometry, each hydrogel was subjected to alternating oscillations at 1% and 1000% strain. The high strain regime disrupted the network, and the low strain regime enabled self-healing of the hydrogel. Similar to the qualitative self-healing study, the pH 7 hydrogels demonstrated complete self-healing while the pH 3 hydrogels did not (Figure S10). The kinetic differences seen between the low and high pH environments show a clear difference in the macroscopic self-healing ability of these hydrogels.

Modulating Hydrogel Stability and Release with Biologically Relevant pH

An important property of dynamic covalent hydrogels is their stability in solution, as the reversible bonds allow the polymer to detach from the hydrogel network and diffuse into solution. To that end, we performed two studies investigating the stability of these hydrogels. We first measured the stability of the hydrogels at each pH value while surrounded by buffer. This environment allowed the hydrogels to swell indefinitely, which increased the rate at which polymer can dissociate from the hydrogel (Figure 5A). As the hydrogel swells, the local concentration of cross-linking groups is decreased, shifting the equilibrium of the reaction to a relatively higher concentration of unbound cross-links (reactants) versus formed cross-links (products). Additionally, this decrease in cross-linking density acts a positive feedback loop, wherein the decrease in cross-links leads to more swelling, which leads to a further decrease in cross-linker concentration. Thus, when considering the swollen mass of a hydrogel, it is anticipated there will be an initial increase in mass as the volume of the hydrogel increases, but the mass will eventually decrease after a significant portion of the polymer diffuses away.

Each of the hydrogels at pH 3−7 demonstrated the trend in mass loss described above (Figure 5B). As the pH increased, the rate of hydrogel mass loss also increased. For instance, at pH 3, it took 2200 min for complete dissolution of the hydrogel, whereas at pH 7, it only took 450 min. In addition to faster bond exchange kinetics at pH 7, the reaction possesses a lower equilibrium constant, as previously mentioned. For a given polymer to diffuse away, either all of the functional groups for a single macromer must be dissociated, or a section of bound macromers must have all of their functional groups dissociated from the hydrogel network. A lower equilibrium constant means that fewer bound cross-links are present in the first place. Additionally, the maximum mass decreased as the pH increased, ranging from approximately a 150% increase in mass for the pH 3 hydrogels to virtually no increase for the pH 7 hydrogels. As discussed previously, as the hydrogel swells, the local cross-linking decreases. Because the cross-links are more stable at lower pH, there is more time for the polymer chains to stretch without becoming detached from the network. Conversely, at high pH values, the cross-links can rapidly break

https://doi.org/10.1021/acspolymersau.1c00049
ACS Polym. Au 2022, 2, 129−136

as the polymer chains stretch, leading to polymer diffusing into solution at an increased rate.

To validate the contributions of swelling toward hydrogel mass loss, a swelling restricted mass loss study was also performed. In this study, 50 μL hydrogels using pH 3 and pH 7 buffers were formed in the bottom of microcentrifuge tubes, and 1.3 mL of the corresponding buffer was placed above each hydrogel. This experimental setup allowed diffusion of the polymer to occur only in one direction, and the walls of the microcentrifuge tube severely restricted the ability of the hydrogel to swell (Figure 5A). As stated previously, swelling in these reversible covalent hydrogels led to accelerated mass loss. However, when swelling was restricted, both hydrogels remained after 100 h (Figure 5C), whereas no hydrogel lasted longer than 38 h in the swelling unrestricted study. Additionally, the pH 7 hydrogels still lost mass at a faster rate than the pH 3 hydrogels, although the difference between the two was significantly less than in the swelling unrestricted study. A control hydrogel cross-linked with an irreversible thiol-ene linkage demonstrated virtually no mass loss in an identical experiment (Figure S11). Based on these results, swelling restriction may be used as a strategy to control the lifespan of these hydrogels.

Using this swelling restricted hydrogel system, we then determined the release profile of an encapsulated model protein, BSA-fluorescein, at pH 3 and pH 7, by measuring the fluorescence of released protein in the surrounding buffer. Due to the reversible nature of the cross-linking, there are two potential methods of release. The first is diffusion of the protein through the hydrogel, which is dictated by the size of the encapsulated protein and the mesh size of the hydrogel. If the encapsulated protein is larger than the mesh size of the hydrogel, it is possible to suppress any diffusional release. The second release method is through degradation of the hydrogel, as the reversible cross-linking allows the polymer to diffuse away from the hydrogel into the surrounding solution. Our results show that the protein was released at a much faster rate in the pH 7 hydrogels versus the pH 3 hydrogels (Figure 5D). Multiple factors contribute to this drastic difference in release. First, the pH 7 hydrogels have a lower equilibrium constant and thus a lower cross-linking density. This leads to an increase in the mesh size of the hydrogel, which allows diffusion of encapsulated protein to occur at a faster rate. Additionally, since the cross-links of the pH 7 hydrogel rearrange much more rapidly than in the pH 3 hydrogel, the pH 7 cross-links can break and re-form around the encapsulated protein much faster. In essence, this would increase the effective rate of diffusion for the protein, as the mobility of the protein is less restricted. Finally, as the mass loss study showed that the pH 7 hydrogels lose mass at a faster rate than the pH 3 hydrogels, any encapsulated protein in the surface portion of the hydrogel that diffuses away from the bulk hydrogel will dissolve into solution. In combination, these factors play a role in the much more rapid protein release profile of the pH 7 hydrogels. In contrast, the release profiles of irreversibly cross-linked thiol-ene hydrogels showed no differences in release at either pH 3 or pH 7, and little release occurred overall for both pH values (Figure S12). These control hydrogels remained static over the course of the experiment, and the high cross-link conversion enabled the mesh size in the hydrogel to approach the minimum mesh size achievable. Taken together, these results demonstrate that pH is an effective manipulator of protein release in these reversible thia-Michael addition cross-linked hydrogels.

CONCLUSION

In this work, we demonstrated the effects of pH on the kinetics, mechanics, and protein release of reversible thia-Michael addition cross-linked hydrogels. Although both the forward and reverse rate constants increased at elevated pH, the equilibrium constant decreased, leading to faster mass loss and release of an encapsulated model protein. The drastic difference in bond exchange kinetics within these hydrogels at pH 3 and pH 7 are promising for applications such as therapeutic release within the gastrointestinal tract, where such pH changes are present. In addition, the strategy of controlling bond exchange kinetics to modulate release offers a complementary mechanism to other pH-responsive hydrogels, which rely on changes in polymer swelling or erosion alone. In summary, these results demonstrate how pH can be leveraged as an effective way to control the properties of hydrogels cross-linked by reversible thia-Michael addition and offer fundamental insight into kinetic control of dynamic covalent hydrogels.

ASSOCIATED CONTENT

Supporting Information

The Supporting Information is available free of charge at https://pubs.acs.org/doi/10.1021/acspolymersau.1c00049.

^{1}H NMR spectra, fluorescence standard curves, UV/vis data, reaction mechanism schematic, strain sweep measurements, crossover point data, stress relaxation measurements, and model calculations (PDF)

AUTHOR INFORMATION

Corresponding Author

Adrianne M. Rosales − *McKetta Department of Chemical Engineering, University of Texas at Austin, Austin, Texas 78712, United States;* orcid.org/0000-0003-0207-7661; Email: arosales@che.utexas.edu

Authors

Thomas M. FitzSimons − *McKetta Department of Chemical Engineering, University of Texas at Austin, Austin, Texas 78712, United States;* orcid.org/0000-0001-7316-475X

Eric V. Anslyn − *Department of Chemistry, University of Texas at Austin, Austin, Texas 78712, United States;* orcid.org/0000-0002-5137-8797

Complete contact information is available at: https://pubs.acs.org/10.1021/acspolymersau.1c00049

Author Contributions

T.M.F., E.V.A., and A.M.R. conceived and designed the research. T.M.F. performed experiments. A.M.R. supervised experiments. The manuscript was written through contributions of all authors. All authors have given approval to the final version of the manuscript.

Notes

The authors declare no competing financial interest.

https://doi.org/10.1021/acspolymersau.1c00049
ACS Polym. Au 2022, 2, 129−136

■ ACKNOWLEDGMENTS

This research was supported by the National Science Foundation (NSF MRSEC DMR-1720595, T.M.F., E.V.A., and A.M.R.) and by the National Institutes of Health (R35GM138193, A.M.R.). The authors acknowledge the use of shared research facilities supported in part by the Texas Materials Institute, the Center for Dynamics and Control of Materials: an NSF MRSEC (DMR-1720595), and the NSF National Nanotechnology Coordinated Infrastructure (ECCS-1542159). We thank Anne Crowell for synthesis of some of the PEG macromers used in this work.

■ REFERENCES

(1) Marco-Dufort, B.; Willi, J.; Vielba-Gomez, F.; Gatti, F.; Tibbitt, M. W. Environment Controls Biomolecule Release from Dynamic Covalent Hydrogels. *Biomacromolecules* **2021**, *22* (1), 146−157.
(2) Yesilyurt, V.; Webber, M. J.; Appel, E. A.; Godwin, C.; Langer, R.; Anderson, D. G. Injectable Self-Healing Glucose-Responsive Hydrogels with PH-Regulated Mechanical Properties. *Adv. Mater.* **2016**, *28* (1), 86−91.
(3) Ding, X.; Li, G.; Zhang, P.; Jin, E.; Xiao, C.; Chen, X. Injectable Self-Healing Hydrogel Wound Dressing with Cysteine-Specific On-Demand Dissolution Property Based on Tandem Dynamic Covalent Bonds. *Adv. Funct. Mater.* **2021**, *31*, 2011230.
(4) FitzSimons, T. M.; Oentoro, F.; Shanbhag, T. V.; Anslyn, E. V.; Rosales, A. M. Preferential Control of Forward Reaction Kinetics in Hydrogels Crosslinked with Reversible Conjugate Additions. *Macromolecules* **2020**, *53* (10), 3738−3746.
(5) Smithmyer, M. E.; Deng, C. C.; Cassel, S. E.; Levalley, P. J.; Sumerlin, B. S.; Kloxin, A. M. Self-Healing Boronic Acid-Based Hydrogels for 3D Co-Cultures. *ACS Macro Lett.* **2018**, *7* (9), 1105−1110.
(6) McKinnon, D. D.; Domaille, D. W.; Cha, J. N.; Anseth, K. S. Biophysically Defined and Cytocompatible Covalently Adaptable Networks as Viscoelastic 3d Cell Culture Systems. *Adv. Mater.* **2014**, *26* (6), 865−872.
(7) Michal, B. T.; Spencer, E. J.; Rowan, S. J. Stimuli-Responsive Reversible Two-Level Adhesion from a Structurally Dynamic Shape-Memory Polymer. *ACS Appl. Mater. Interfaces* **2016**, *8*, 11041−11049.
(8) Herbert, K. M.; Dolinski, N. D.; Boynton, N. R.; Murphy, J. G.; Lindberg, C. A.; Sibener, S. J.; Rowan, S. J. Controlling the Morphology of Dynamic Thia-Michael Networks to Target Pressure-Sensitive and Hot Melt Adhesives. *ACS Appl. Mater. Interfaces* **2021**, *13*, 27471−27480.
(9) Kloxin, C. J.; Bowman, C. N. Covalent Adaptable Networks: Smart, Reconfigurable and Responsive Network Systems. *Chem. Soc. Rev.* **2013**, *42*, 7161−7173.
(10) Herbert, K. M.; Getty, P. T.; Dolinski, N. D.; Hertzog, J. E.; de Jong, D.; Lettow, J. H.; Romulus, J.; Onorato, J. W.; Foster, E. M.; Rowan, S. J. Dynamic Reaction-Induced Phase Separation in Tunable, Adaptive Covalent Networks. *Chem. Sci.* **2020**, *11*, 5028−5036.
(11) Lou, J.; Liu, F.; Lindsay, C. D.; Chaudhuri, O.; Heilshorn, S. C.; Xia, Y. Dynamic Hyaluronan Hydrogels with Temporally Modulated High Injectability and Stability Using a Biocompatible Catalyst. *Adv. Mater.* **2018**, *30*, 1705215.
(12) Zhang, B.; Digby, Z. A.; Flum, J. A.; Chakma, P.; Saul, J. M.; Sparks, J. L.; Konkolewicz, D. Dynamic Thiol-Michael Chemistry for Thermoresponsive Rehealable and Malleable Networks. *Macromolecules* **2016**, *49* (18), 6871−6878.
(13) Cromwell, O. R.; Chung, J.; Guan, Z. Malleable and Self-Healing Covalent Polymer Networks through Tunable Dynamic Boronic Ester Bonds. *J. Am. Chem. Soc.* **2015**, *137* (20), 6492−6495.
(14) Accardo, J. V.; Kalow, J. A. Reversibly tuning hydrogel stiffness through photocontrolled dynamic covalent crosslinks. *Chemical Science* **2018**, *9*, 5987−5993.
(15) Mckinnon, D. D.; Domaille, D. W.; Cha, J. N.; Anseth, K. S. Bis-Aliphatic Hydrazone-Linked Hydrogels Form Most Rapidly at Physiological PH: Identifying the Origin of Hydrogel Properties with Small Molecule Kinetic Studies. *Chem. Mater.* **2014**, *26*, 2382−2387.
(16) Marco-Dufort, B.; Iten, R.; Tibbitt, M. W. Linking Molecular Behavior to Macroscopic Properties in Ideal Dynamic Covalent Networks. *J. Am. Chem. Soc.* **2020**, *142* (36), 15371−15385.
(17) George, M.; Abraham, T. E. PH Sensitive Alginate-Guar Gum Hydrogel for the Controlled Delivery of Protein Drugs. *Int. J. Pharm.* **2007**, *335* (1−2), 123−129.
(18) Krishna Rao, K. S. V.; Ha, C. S. PH Sensitive Hydrogels Based on Acryl Amides and Their Swelling and Diffusion Characteristics with Drug Delivery Behavior. *Polym. Bull.* **2009**, *62* (2), 167−181.
(19) Huang, Y.; Yu, H.; Xiao, C. PH-Sensitive Cationic Guar Gum/Poly (Acrylic Acid) Polyelectrolyte Hydrogels : Swelling and in Vitro Drug Release. *Carbohydr. Polym.* **2007**, *69*, 774−783.
(20) am Ende, M. T.; Hariharan, D.; Peppas, N. A. Factors Influencing Drug and Protein Transport and Release from Ionic Hydrogels. *React. Polym.* **1995**, *25*, 127−137.
(21) Brannon-peppas, L.; Peppas, N. A. Equilibrium Swelling Behavior of Dilute Ionic Hydrogels in Electrolytic Solutions. *J. Controlled Release* **1991**, *16*, 319−330.
(22) Guo, Z.; Ma, W.; Gu, H.; Feng, Y.; He, Z.; Chen, Q.; Mao, X.; Zhang, J.; Zheng, L. PH-Switchable and Self-Healable Hydrogels Based on Ketone Type Acylhydrazone Dynamic Covalent Bonds. *Soft Matter* **2017**, *13*, 7371−7380.
(23) Seidler, C.; Ng, D. Y. W.; Weil, T. Native Protein Hydrogels by Dynamic Boronic Acid Chemistry. *Tetrahedron* **2017**, *73* (33), 4979−4987.
(24) Wu, D.; Shi, X.; Zhao, F.; Chilengue, S. T. F.; Deng, L.; Dong, A.; Kong, D.; Wang, W.; Zhang, J. An Injectable and Tumor-Specific Responsive Hydrogel with Tissue- Adhesive and Nanomedicine-Releasing Abilities for Precise Locoregional Chemotherapy. *Acta Biomater.* **2019**, *96*, 123−136.
(25) Nair, D. P.; Podgorski, M.; Chatani, S.; Gong, T.; Xi, W.; Fenoli, C. R.; Bowman, C. N. The Thiol-Michael Addition Click Reaction: A Powerful and Widely Used Tool in Materials Chemistry. *Chem. Mater.* **2014**, *26*, 724−744.
(26) Dirksen, A.; Dirksen, S.; Hackeng, T. M.; Dawson, P. E. Nucleophilic Catalysis of Hydrazone Formation and Transimination : Implications for Dynamic Covalent Chemistry. *J. Am. Chem. Soc.* **2006**, *128*, 15602−15603.
(27) Rehmann, M. S.; Skeens, K. M.; Kharkar, P. M.; Ford, E. M.; Maverakis, E.; Lee, K. H.; Kloxin, A. M. Tuning and Predicting Mesh Size and Protein Release from Step Growth Hydrogels. *Biomacromolecules* **2017**, *18* (10), 3131−3142.
(28) Parada, G. A.; Zhao, X. Ideal Reversible Polymer Networks. *Soft Matter* **2018**, *14* (25), 5186−5196.

https://doi.org/10.1021/acspolymersau.1c00049
ACS Polym. Au 2022, 2, 129−136